

Supporting Information

Accelerated DNAzyme-based fluorescent nanoprobe for highly sensitive microRNA detection in live cells

Yanan Wu,^a Hong-Min Meng,^{*a} Juan Chen,^a Kemei Jiang,^a Ran Yang,^a Yingying Li,^a
Ke Zhang,^b Lingbo Qu,^{*a} Xiao-Bing Zhang,^c and Zhaohui Li^{*a}

^a *Institute of Chemical Biology and Clinical Application at the First Affiliated Hospital, Henan Joint International Research Laboratory of Green Construction of Functional Molecules and Their Bioanalytical Applications, College of Chemistry, Zhengzhou University, Zhengzhou 450001, P.R. China*

^b *Department of Chemistry and Chemical Biology, Northeastern University, Boston, MA 02115, United States.*

^c *College of Chemistry and Chemical Engineering, Hunan University, Changsha 410082, P.R. China*

* Corresponding authors. Tel.: +86-371-67780037.

E-mail address: hmmeng2017@zzu.edu.cn (H. M. Meng), qulingbo@zzu.edu.cn (L. B. Qu) and zhaohui.li@zzu.edu.cn (Z. H. Li).

Table of contents:

Experimental Section	S3
Table S1. Oligonucleotide sequences	S6
Table S2. Comparison of reaction time and sensitivity of different miR-21 detection methods	S7
Figure S1. Analysis of the secondary structure of the hairpin probe	S8
Figure S2. Gel electrophoresis image of accelerated-DzFN	S9
Figure S3. Optimization of the reaction buffer	S10
Figure S4. Optimization of the concentration of Mg ²⁺	S11
Figure S5. Comparison of fluorescence intensity between DzFN and accelerated-DzFN ..	S12
Figure S6. <i>In vitro</i> fluorescence response of DzFN	S13
Figure S7. <i>In vitro</i> fluorescence response of H1	S14
Figure S8. Comparison of the reaction area and local concentration of two hairpin probes for DzFN and accelerated-DzFN	S15
Figure S9. Stability assay	S16
Figure S10. Fluorescence response of accelerated-DzFN treated with DNase I	S17
Figure S11. Cytotoxicity assay	S18
Figure S12. Fluorescence colocalization analysis	S19
Figure S13. 3D fluorescence imaging	S20
Figure S14. Optimization of the incubation time in living cells	S21
Figure S15. Fluorescence images of accelerated-DzFN sense the changes of miR-21 expression levels in MCF-7 cells	S22
Reference	S23

Experimental Section

Chemicals and Materials.

Cell culture media DMEM and SYBR Gold were gained from Thermo Scientific HyClone (USA). Acrylamide/Bis solution (30% (w/v)), Cell Counting Kit-8, Hoechst 33342 and PBS buffer were obtained from Sangon Biotech Co., Ltd. (Shanghai, China). All the chemicals were of analytical grade and used without further treatment. All aqueous solutions were prepared using DEPC-treated ultrapure water ($\geq 18 \text{ M}\Omega$, Milli-Q, Millipore). All oligonucleotides were synthesized by Sangon Biotech Co., Ltd. (Shanghai, China) and purified by high-performance liquid chromatography (HPLC). The sequences of the oligonucleotides are listed in **Table S1**.

Apparatus.

All the fluorescence measurements were carried out at 37 °C in a Hitachi F-7100 fluorescence spectrometer (Japan). All cells were incubated by using a Thermo FORMA 3111 CO₂ incubator (Thermo Fisher, USA). All fluorescence images of cells were acquired by a Leica TCS SP8 confocal laser scanning fluorescence microscope (Leica, Germany).

Preparation of accelerated-DzFN.

H1 and H2 were separately added to the 20 mM Tris-HCl buffer (140 mM NaCl, pH 7.4) being heated to 95 °C for 5 min, then cooled to room temperature to form hairpin structure. A1 and A2 were annealed in Tris-HCl buffer at 95 °C for 5 min and cooled to room temperature slowly over 4 h to form stable DNA nanowire. The accelerated-DzFN was prepared by the equimolar mixing a mixture of DNA nanowire, H1 and H2 for 2 h at 37 °C.

Preparation of reaction buffer.

20 mM Tris-HCl (pH 7.4): 20 mM Tris-base, 140 mM NaCl; 20 mM HEPES (pH 7.4): 20 mM HEPES, 140 mM NaCl; 10 mM PBS (pH 7.4): 140 mM NaCl, 2.7 mM KCl, 10 mM NaH₂PO₄·2H₂O; SPSC (pH 7.4): 1 M NaCl, 50 mM Na₂HPO₄·12H₂O.

Gel electrophoresis experiments.

The DNAzyme cleavage reaction was performed using 12% native polyacrylamide gel electrophoresis (PAGE) in 1×TBE buffer. 1 μM H1 and 0.5 μM DNA target were mixed with 1 μM H2 and incubated for 2 h at 37 °C. Successful formation of accelerated-DzFN was verified by 3% agarose gel electrophoresis. The

electrophoresis was run at a constant potential of 80 V for 40 min after loading 10 μ L of each sample into the lanes.

***In vitro* fluorescence experiments.**

Fluorescence experiments were carried out with excitation wavelength at 488 nm and emission between 510 nm and 650 nm. The slit width was set to be 5 nm for the excitation and 5 nm for the emission. For each experiment, 100 nM accelerated-DzFN was mixed in a 95 μ L Tris-HCl buffer solution, and 5 μ L of miR-21 at a certain concentration were then added to initiate the DNAzyme cleavage reaction at 37 °C. The fluorescence kinetics analysis was carried out on recording the fluorescence signal of 522 nm at 10 min intervals. For selectivity test, a certain concentration of non-target miRNAs and mutation targets were added into the probe, respectively. The measuring processing was as the same as above.

Cell culture.

MCF-7 (human breast cancer cell line), HepG2 (human hepatocellular liver carcinoma cell line), HeLa (human cervical cancer cell line) and HL-7702 (human hepatocyte cell line) cells were cultured in Dulbecco's modified Eagle's medium (DMEM) supplemented with 10 % fetal calf serum, 100 μ g·mL⁻¹ penicillin, and 100 μ g·mL⁻¹ streptomycin at 37 °C in a humidified 5 % CO₂-containing atmosphere. Phosphate-Buffered Saline (PBS) (pH 7.4, Ca²⁺ and Mg²⁺ free) was used to wash cells.

Stability assay.

To test the stability of the probe in complex matrix, 100 nM accelerated-DzFN was incubated with 20% fetal bovine serum, 2U/mL DNase I and HL-7702 cell lysate at 37 °C. Real-time recording of FAM fluorescence changes at 522 nm with 488 nm excitation. HL-7702 cell lysate was obtained as follows: The HL-7702 cells were cultured in a humidified incubator for 24 h, and then the cells were broken using an ultrasonic cell crusher for about 5 min. Finally, the cell lysate was immediately used for the stability assay without centrifugation.

Confocal laser scanning microscopy (CLSM) experiments.

All cell lines were cultured in a 20 mm confocal dish and incubated for 24 h to reach 70-80%. Next, the cells were incubated with 50 nM accelerated-DzFN for 4 h at 37 °C, washed with PBS three times before imaging. The fluorescence images were taken under 63 \times oil-immersion objective and an Ar⁺ laser was used as an excitation source. The FAM fluorescence image was recorded in green channel with 488 nm excitation. For fluorescence colocalization imaging, the MCF-7 cells were incubated

with 50 nM accelerated-DzFN, then the cells were treated with 200 μ L Hoechst 33342 for 20 min. Excitation of Hoechst 33342 was carried out at 405 nm and emissions were collected in the blue channel. To detect the dynamic changes of miR-21 in cells, two groups of MCF-7 cells were transfected with anti-miR-21 (300 nM) and miR-21 mimics (300 nM) for 2 h, respectively, the untreated group served as the control. For investigation of the expression levels of miR-21 in different cells, MCF-7, HepG2, HeLa and HL-7702 cells were prepared. All cells were first incubated with 50 nM accelerated-DzFN for 4 h, then washed and imaged. All the mean fluorescence intensities were presented after processing by Image J software.

Cytotoxicity assay.

MCF-7 cells were seeded in a 96 well plates at a density of 1×10^5 cells per well. After 24 h incubation, the cells were treated with 100 μ L of cell medium containing accelerated-DzFN at different concentrations and incubated for 24 h. After incubation, the cell medium was replaced with 100 μ L fresh cell medium containing Cell Counting Kit-8 solution to each well for 2 h. The cell viability was determined by measuring the absorbance at 450 nm by a Spark multi-detection microplate reader (Austria).

Table S1. Oligonucleotide sequences used in this work

Name	Sequence (5'-3')
A1	ATCTTATTAGTCGTCTCGTTCGTTAAATGGTCAGAAATA TGGGTTCCATGGTGTTTATGATATGAAGTGTTGGAG
A2	ATTCTAATTAGGACAAACCCATATTTCTGACCATTTAAC GAACGACTCCAACACTTCATATCATAAACACCATGG
H1	GACGACTAATAAGATTCAACATCAGT(BHQ1)CTGATAA GCGCGCTCTCAT/ <i>rA</i> /G GCGCTTATCAGACT-FAM
H2	TGTCCTAATTAGAATATAAGCGCTCCGAGCCGGTCGAA ATGAGAGCGCGCTTATCAGACACCGGCTCGGAG
DNA target	TAGCTTATCAGACTGATGTTGA
miR-21	UAGCUUAUCAGACUGAUGUUGA
single-base mismatch	UAGCUUAUCACACUGAUGUUGA
two-base mismatch	UCGCUUAUCACACUGAUGUUGA
three-base mismatch	UCGCUUAUCAGACGGAUCUUGA
miR-141	UAACACUGUCUGGUAAAGAUGG
let-7d	AGAGGUAGUAGGUUGCAUAGUU
miR-21 mimics	TAGCTTATCAGACTGATGTTGA
anti-miR-21	TCAACATCAGTCTGATAAGCTA

The *rA* denotes RNA base. The bases that different from those in miR-21 are highlighted in blue.

Table S2. The comparison of our method with other miR-21 detection methods in terms of reaction time and sensitivity *in vitro*.

Method	Probe carrier	Reaction time (h)	Detection limit (nM)	Ref.
DNAzyme-based amplification	Gold nanoparticle	8	0.025	1
Strand displacement reaction	DNA nanostructure	4	0.061	2
Strand displacement reaction	Gold nanoparticle	6	0.0045	3
Entropy-driven catalytic reaction	Gold nanoparticle	1	0.008	4
Catalytic hairpin assembly	Gold nanoparticle	4	0.067	5
DNAzyme reaction	Zeolitic imidazolate framework-8	2	0.68	6
Hybridization chain reaction	MnO ₂ nanosheets	3.3	0.0098	7
Accelerated-DzFN	DNA nanowire	0.33	0.0012	This work

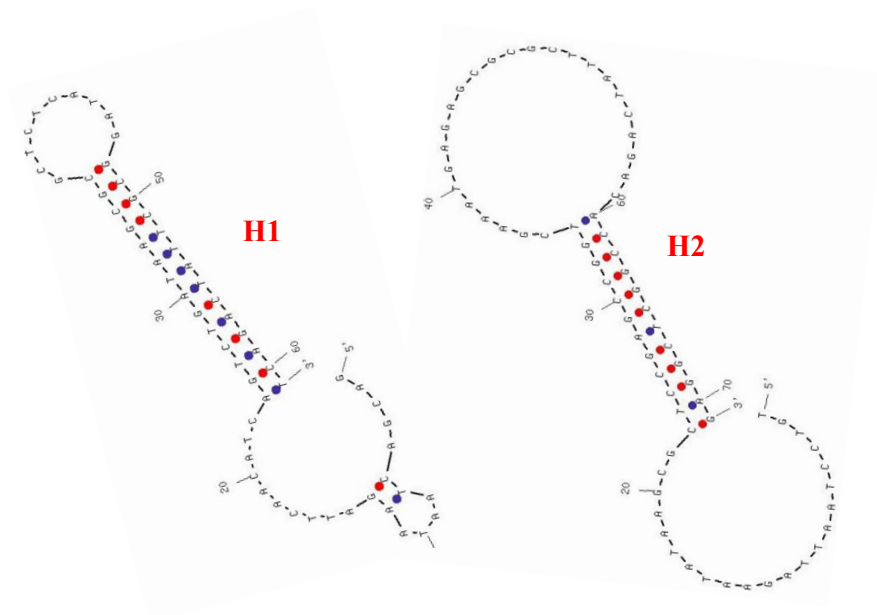


Figure S1. Analysis of the secondary structure of the hairpin probe (<http://sg.idtdna.com>). The hairpin probe consists of a stem, a loop and a bare toehold.

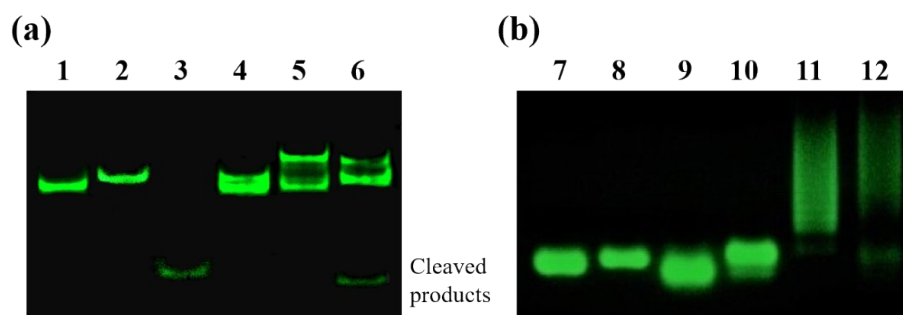


Figure S2. Gel electrophoresis image of accelerated-DzFN. (a) Validation of the DNAzyme catalytic activity by native polyacrylamide gel electrophoresis. Lane 1: H1; Lane 2: H2; Lane 3: miR-21; Lane 4: H1+H2; Lane 5: H1+miR-21; Lane 6: H1+H2+miR-21+Mg²⁺; (b) Agarose gel electrophoresis image of self-assembled accelerated-DzFN. Lane 7: A1; Lane 8: A2; Lane 9: H1; Lane 10: H2; Lane 11: A1+A2; lane 12: A1+A2+H1+H2.

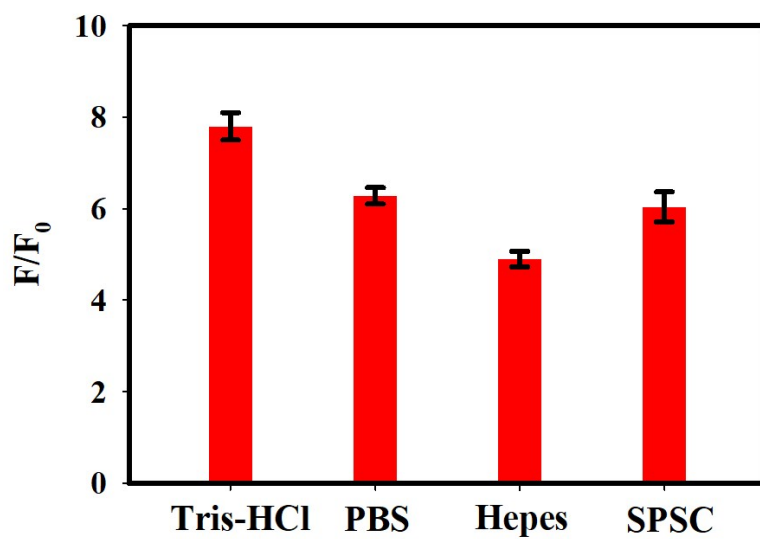


Figure S3. Optimization of the reaction buffer. F and F_0 is the fluorescence intensity of the accelerated-DzFN in the presence and absence of 50 nM miR-21, respectively. The error bars indicate mean \pm SD ($n = 3$).

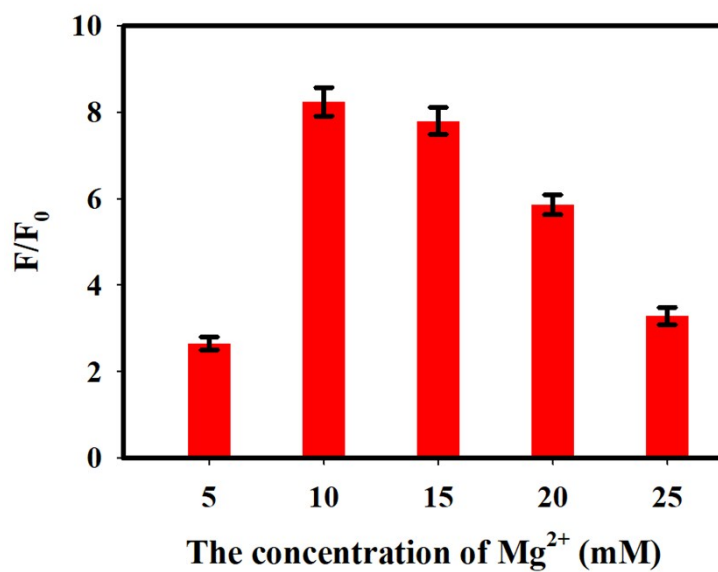


Figure S4. Optimization of the concentration of Mg²⁺. F and F₀ is the fluorescence intensity of the accelerated-DzFN in the presence and absence of 50 nM miR-21, respectively. The error bars indicate mean ± SD (n = 3).

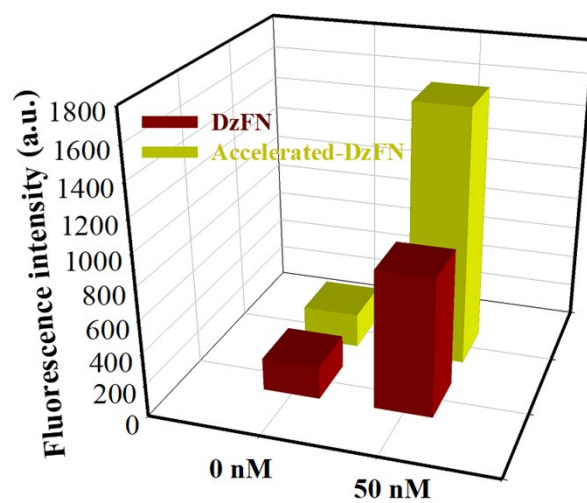


Figure S5. Comparison of fluorescence intensity between accelerated-DzFN and DzFN responding to 50 nM miR-21.

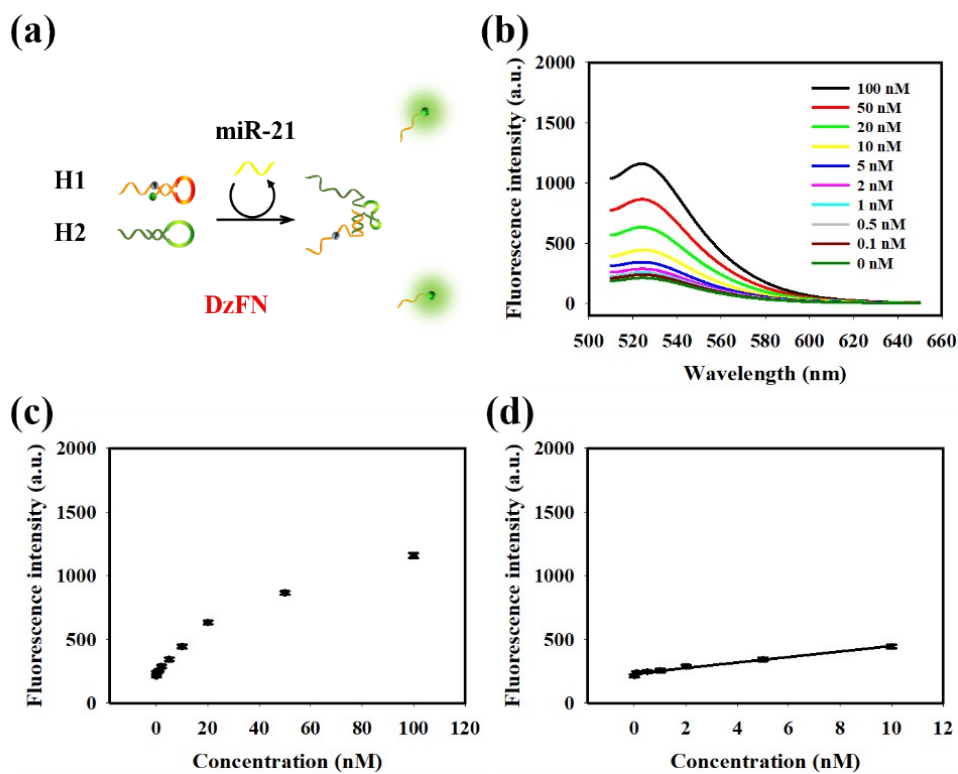


Figure S6. *In vitro* fluorescence response of DzFN. (a) Schematic and (b) fluorescence emission spectra of DzFN with various concentration of miR-21 and (c) corresponding calibration curves. (d) show the calibration curves at the low concentration range. The error bars indicate means \pm SD (n = 3).

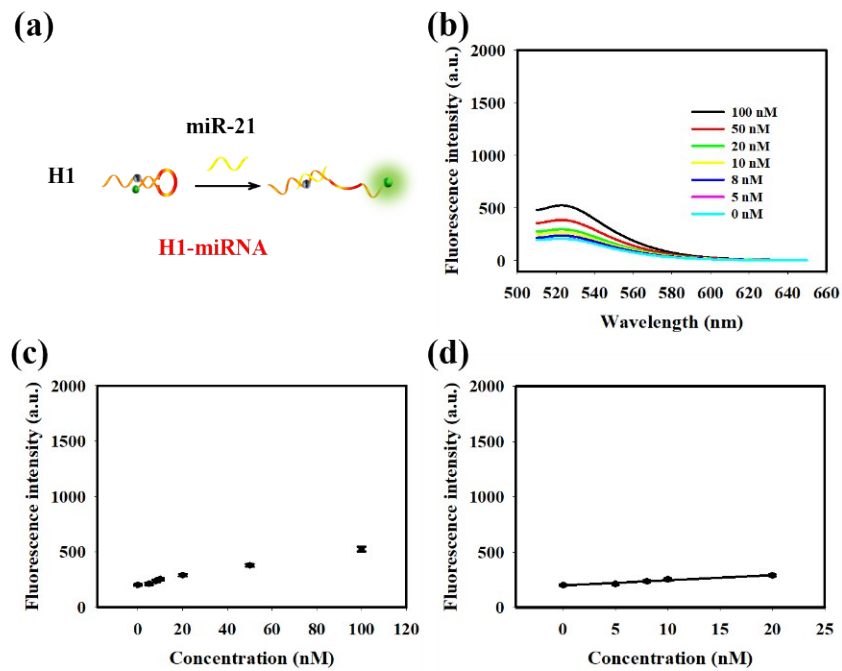


Figure S7. *In vitro* fluorescence response of H1. (a) Schematic and (b) fluorescence emission spectra of H1-miRNA respond to various concentration of miR-21 and (c) corresponding calibration curves. (d) show the calibration curves at the low concentration range. The error bars indicate means \pm SD ($n = 3$).

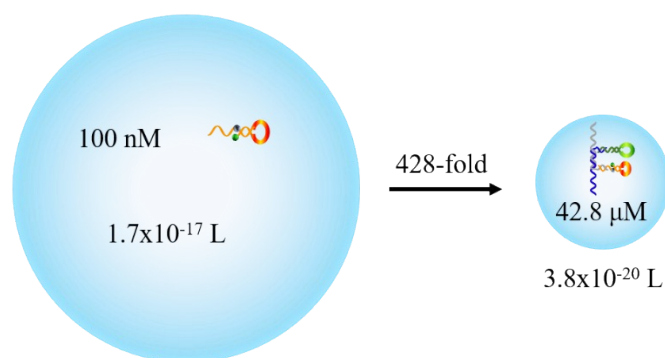


Figure S8. Comparison of the reaction area and local concentration of two hairpin probes for DzFN and accelerated-DzFN.

We used the equation $V = 1/cN$ to estimate the volume of the reaction sphere using the concentrations of the probes, in which c is the concentration of the hairpin probe, and N represents the Avogadro constant. For the free DzFN with 100 nM each of H1 and H2, the volume of the sphere containing DNA hairpin probe was calculated to be 1.7×10^{-17} L with a radius of 157 nm. For the accelerated-DzFN, the distance between the two hairpin probes was about 20.3 nm (60 bp) and the local concentrations was calculated to be 42.8 μ M, which was increased 428-fold compared to the reaction in the bulk condition. Because the reaction speed is highly related with collision frequency, the increased local concentration of H1 and H2 significantly enhanced the collision frequency of two hairpin probes, causing improved reaction time and enchanted catalytic efficiency.

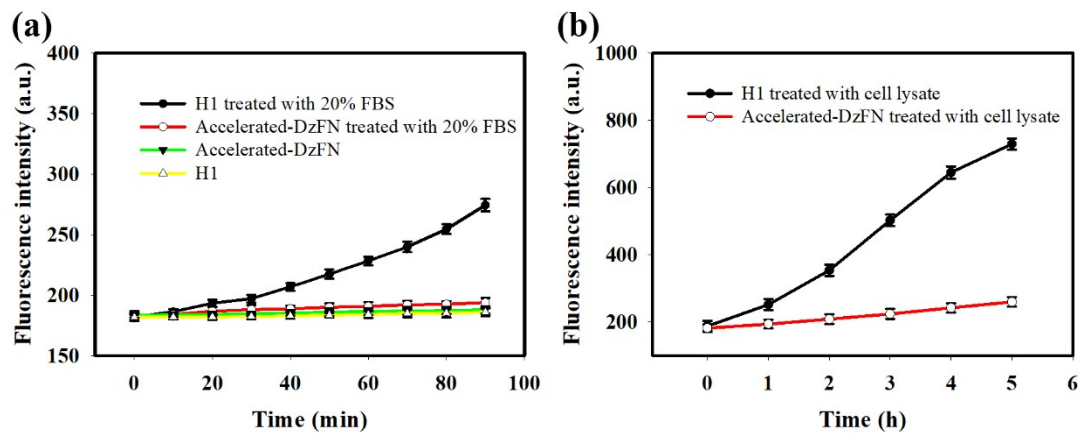


Figure S9. The stability assay of the probes over time in (a) 20% fetal bovine serum (FBS) and (b) HL-7702 cell lysate. The error bars indicate means \pm SD (n = 3).

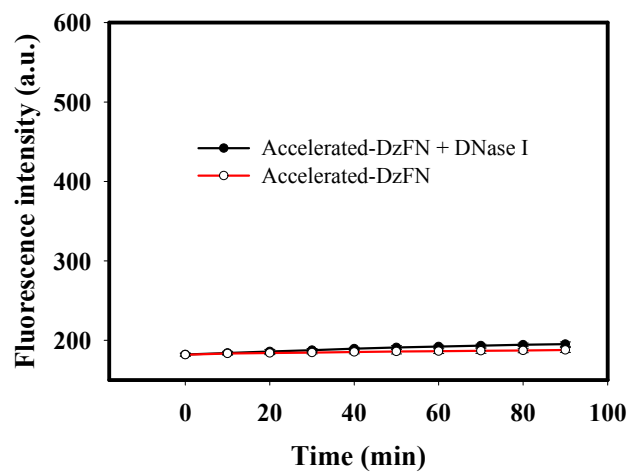


Figure S10. Fluorescence response of accelerated-DzFN treated with 2 U/L DNase I (enzyme deoxyribonuclease I, a common endonuclease capable of effectively cutting both single and double-strand DNA).

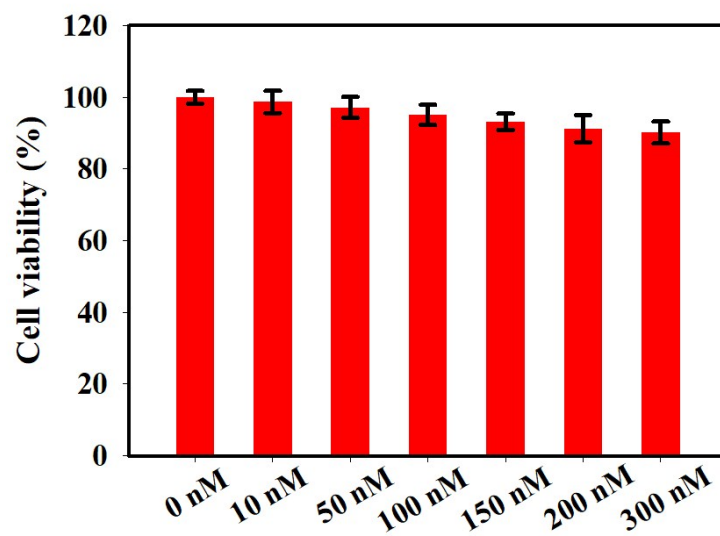


Figure S11. Cytotoxicity assay with different concentrations of accelerated-DzFN. MCF-7 cells were incubated with various concentrations of accelerated-DzFN for 24 h. The error bars indicate means \pm SD (n = 3).

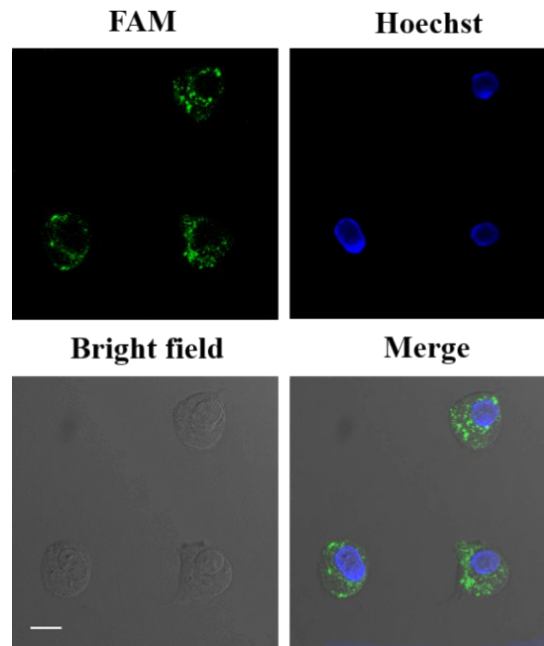


Figure S12. Fluorescence colocalization analysis. MCF-7 cells were incubated with 50 nM accelerated-DzFN (green channel), then treated with 5 mg/mL Hoechst 33342 (blue channel). Scale bar: 15 μ m.

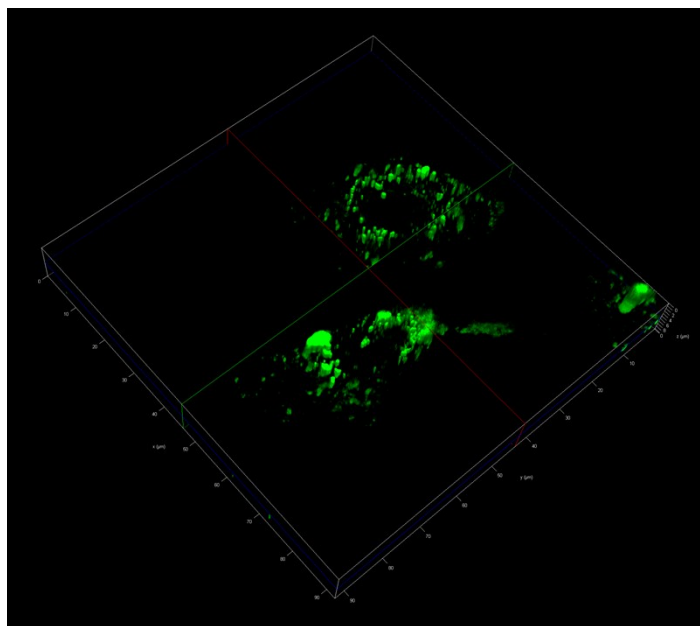


Figure S13. Three-dimensional (3D) fluorescence imaging of miR-21 in MCF-7 cells. The MCF-7 cells were incubated with 50 nM accelerated-DzFN for 4 h at 37 °C.

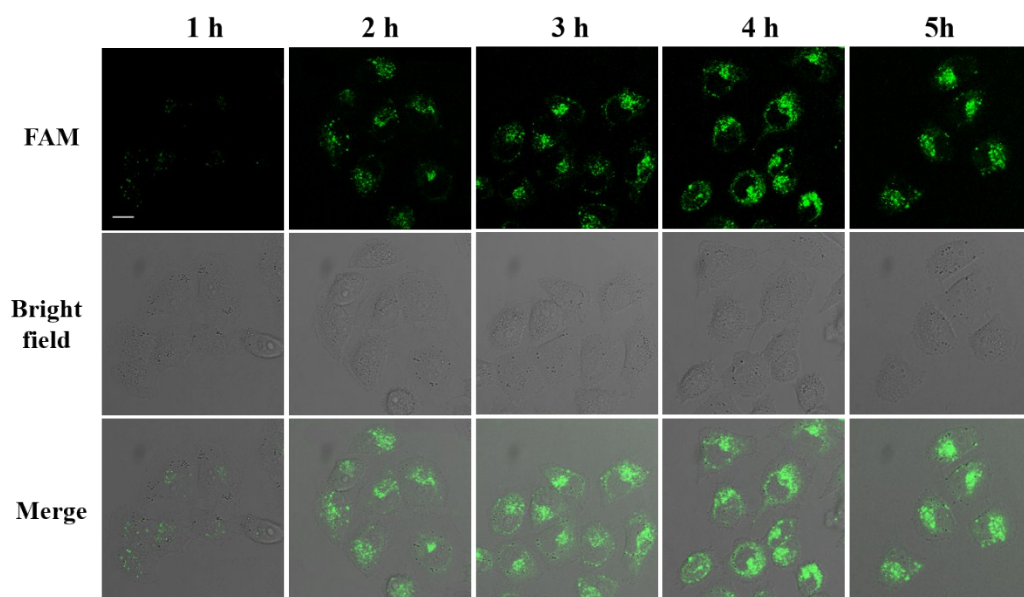


Figure S14. Optimization of the incubation time in living cells. The MCF-7 cells were treated with 50 nM accelerated-DzFN for 1, 2, 3, 4 and 5 h at 37 °C. The imaging was performed with 63×oil immersion objective. The FAM fluorescence emission was collected under an excitation of 488 nm. Scale bar is 15 μ m.

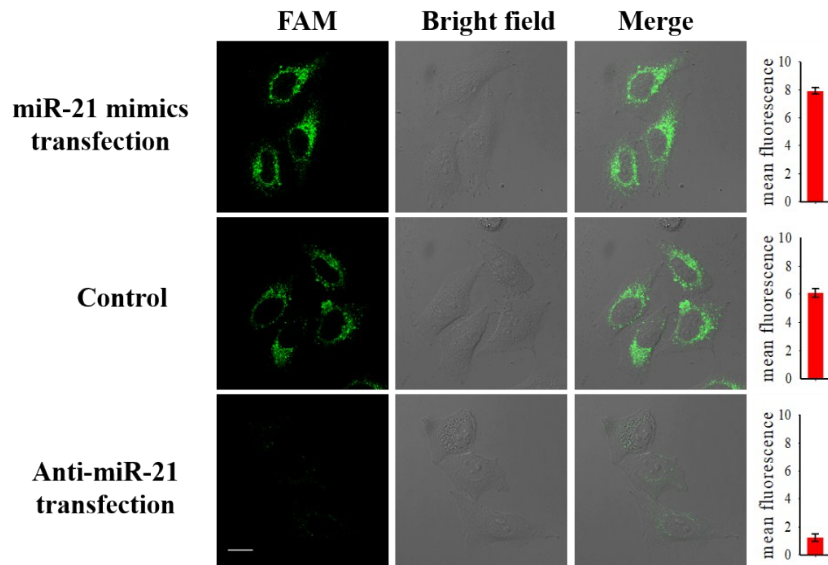


Figure S15. Fluorescence images of accelerated-DzFN sense the changes of miR-21 expression levels in MCF-7 cells. The MCF-7 cells were pretreated with 300 nM miR-21 mimics and anti-miR-21 for 2 h, respectively. Untreated MCF-7 cells were used as the control group. Scale bar is 15 μ m. The error bars represent the standard deviation of three independent measurements.

Reference:

- 1 Y. Yang, J. Huang, X. Yang, X. He, K. Quan, N. Xie, M. Ou, K. Wang, *Anal. Chem.* 2017, **89**, 5850-5856.
- 2 Z. Yang, S. Zhang, H. Zhao, H. Niu, Z. Wu, H. Chang, *Anal. Chem.* 2018, **90**, 13891-13899.
- 3 X. He, T. Zeng, Z. Li, G. Wang, N. Ma, *Angew. Chem. Int. Ed.* 2016, **55**, 3073-3076.
- 4 C. Liang, P. Ma, H. Liu, X. Guo, B. Yin, B. Ye, *Angew. Chem. Int. Ed.* 2017, **56**, 9077-9081.
- 5 J. Wang, J. Huang, K. Quan, J. Li, Y. Wu, Q. Wei, X. Yang, K. Wang, *Chem. Commun.*, 2018, **54**, 10336-10339.
- 6 J. Yi, T. Chen, J. Huo, X. Chu, *Anal. Chem.*, 2017, **89**, 12351-12359.
- 7 M. Ou, J. Huang, X. Yang, X. He, K. Quan, Y. Yang, N. Xie, J. Li, K. Wang, *ChemBioChem*, 2018, **19**, 147-152.